View metadata, citation and similar papers at core.ac.uk
brought to you by CORE

Motor Drive Stabilization in its Chaotic Region

Péter Stumpf[1)], István Nagy [1)]
[1)] Budapest University of Technology and Economics
Department of Automation and Applied Informatics, Budapest, Hungary, {stumpf,nagy}@get.bme.hu

Abstract— **The paper is concerned with the stability analysis and the control of chaos in a permanent magnet dc drive system. The stability analysis is based on the eigenvalues of the Jacobian matrix of the Poincare Map Function (PMF). Using the auxiliary state vector, the Jacobian matrix can be determined without the derivation of the PMF. A compensating ramp signal is used to avoid bifurcation. The slope of the ramp signal is also determined by the auxiliary state vector. The results are verified by computer simulations in the time domain.**

Keywords—DC machines, Speed Control, Nonlinear Dynamics

I. INTRODUCTION

Large number of power electronic circuits belongs to the variable structure piecewise-linear systems. They change their structure after each switching and the sequence of structures succeeds each other periodically in periodic steady-state. Assuming ideal components these structures can be modeled by time-invariant linear models therefore the systems are piecewise-linear. The overall systems are nonlinear due to the dependence of the switching instants on state and input variables, or in some other cases due to saturations or other nonlinearities.

The paper is concerned with the stability analysis and the control of chaos in a commonly used DC drive system, the buck-chopper-fed two-quadrant permanent-magnet DC motor drive (Fig.1). Chan et. al. showed in [1] that, this drive system using a proportional speed controller generally exhibit chaotic behavior. In this paper a PI controller is applied to eliminate the steady-state error. In [4] the Filippov's-method is used to analyze the instabilities of a DC motor drive with a full-bride converter. Similar to [1] also proportional speed controller is used in [4].

The stability study used in the paper is based on the eigenvalues of the Jacobian matrix of the Poincare Map Function (PMF) determined at a fixed point of the system [2]. From the physical viewpoint, it is equivalent to study the behavior of the periodic steady-state trajectory of the system in the state space when it is forced to leave the trajectory to a new orbit by a small deviation from the original trajectory.

In the present paper the Jacobian matrix is determined without the derivation of the PMF itself by applying the auxiliary state vector proposed in [3]. The method uses small differences of state vectors compared to their steady-state values at the start and end of periods and at the switching instant. The Jacobian matrix is obtained directly from the relations among the small differences of the state vectors. The auxiliary state vector preserves the constant switching instants depending on state variables even after the small excursion of the state variables from the steady state.

It is important to note that in linear systems theory the loss of stability implies that the state diverges without limit [5]. However in nonlinear systems the outcome of a stability loss, or in other words bifurcation, does not lead to an unlimited explosion of the variables.

To compensate the instabilities and to expand the stable operation ranges in nonlinear system are a hotspot in power electronics [4]-[11]. In [4] a sinusoidal signal is added to the speed reference signal to extend the parameter range for stable period-1 operation. In the paper, similar to [9] a periodic ramp signal is used. The slope of the ramp signal is determined by using the auxiliary state vector.

II. CURRENT CONTROLLED DC DRIVE SYSTEM

The schematic block diagram of the two-quadrant buck-chopper-fed permanent magnet DC motor drive is shown in Fig. 1. The speed and current control signals can be expressed as (the ramp signal with dotted line now is omitted)

$$y(t) = K_p(\Omega_{ref} - \Omega) + \frac{K_p}{T_i}\int(\Omega_{ref} - \Omega)dt \quad (1)$$

$$u(t) = A_i i(t) \quad (2)$$

where $i(t)$ is the armature current of the motor, $\Omega(t)$ is the speed of the rotor, Ω_{ref} is the reference speed, A_i is the current gain, K_p is the proportional gain and T_i is the integral time constant of the PI controller.

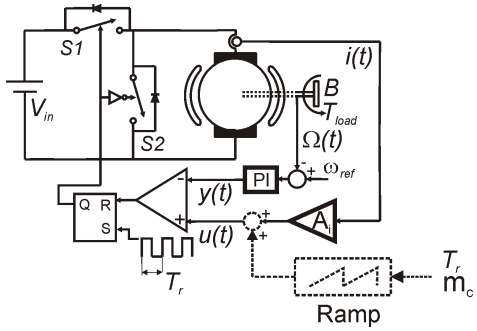

Figure 1. Current controlled DC drive

Both $u(t)$ and $y(t)$ are fed into a comparator. Its output signal is connected to the reset and the clock pulse with period T_r to the set terminal of the *RS* latch. Both power switches are controlled by this RS latch. Once the latch is set by the clock pulse, S1 is turned on and S2 is turned

off until the *u(t)* signal exceeds *y(t)* and then the RS latch is reset. The switch S1 remains open until the arrival of the next clock pulse, while S2 is on.

The DC drive is a variable-structure piecewise-linear system. After each switch, another linear circuit arrangement emerges and the sequence of linear circuits is repeated in the next T_r period. Fig.2 shows the time sequence of structure changes. The duration of structure 1 and 2 is τ_1 and $\tau_2=T_r-\tau_1$, respectively.

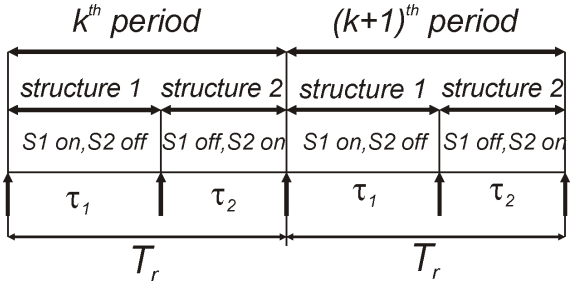

Figure 2. Sequence of structures in steady-state

The switching condition according to Fig.1

$$y(\tau_1)=u(\tau_1) \tag{3}$$

As the switching condition depends on the external speed reference and the internal state vector the DC drive exhibits nonlinear dynamics.

III. MATHEMATICAL BACKGROUND

The behaviour of the DC drive between two switching instants can be modelled with the general state-space representation:

$$\underline{v}(t)=\dot{\underline{x}}(t)=\underline{\underline{A}}_j\,\underline{x}(t)+\underline{\underline{B}}_j\,\underline{g}(t) \tag{4}$$

where *j=1,2* is the structure number, $\underline{x}^T=[\Omega \quad i]$ is the state vector with state variables, $\underline{v}(t)$ is the velocity vector, $\underline{g}^T=[T_{load} \quad V_{in}]$ is the input vector, $\underline{\underline{A}}_j$ and $\underline{\underline{B}}_j$ are the parameter matrix $\underline{\underline{A}}_1=\underline{\underline{A}}_2=\begin{bmatrix}-B/J & K_T/J\\ -K_E/L_a & -R_a/L_a\end{bmatrix}$, $\underline{\underline{B}}_1=\begin{bmatrix}-1/J & 0\\ 0 & 1/L_a\end{bmatrix}$, $\underline{\underline{B}}_2=\begin{bmatrix}-1/J & 0\\ 0 & 0\end{bmatrix}$.

Here V_{in} is the input voltage, T_{load} is the loading torque, B is the viscous damping, J is the inertia, K_E is the back-EMF constant, K_T is the torque constant, R_a and L_a is the armature resistance and inductance, respectively.

Let time τ elapse from the last switching instant. The behaviour of the system in time domain between two switching instants can be described by the solution of (4). Starting the system from $\underline{x}_s=\underline{x}(0)$ and assuming constant input vector the time function of the state-vector is

$$\underline{x}(\tau)=e^{\underline{\underline{A}}_j(\tau)}\underline{x}_s+\int_0^{\tau}e^{\underline{\underline{A}}_j\vartheta}d\vartheta\,\underline{\underline{B}}_j\,\underline{g}(\tau)=\underline{\underline{W}}_j(\tau)\underline{x}_s+\underline{\underline{M}}_j(\tau)\underline{\underline{B}}_j\,\underline{g}(t) \tag{5}$$

where $\underline{\underline{W}}_j$ is the weighting or base matrix. When $\underline{\underline{A}}_j$ is a regular matrix

$$\underline{\underline{M}}_j(\tau)=\underline{\underline{A}}_j^{-1}\left[\underline{\underline{W}}_j(\tau)-\underline{\underline{I}}\right] \tag{6}$$

where $\underline{\underline{I}}$ is the identity matrix with the same size of $\underline{\underline{A}}_j$. For singular $\underline{\underline{A}}_j$ matrix the Taylor series of the matrix exponential function can be used to calculate the integral [2].

In steady state, the values of the state vector at the start of *(k+1)*th period and at the end of *k*th period denoted by suffix *s* and *e*, respectively are equal

$$\underline{x}_{(k+1)1,s}=\underline{x}_{k2,e} \tag{7}$$

Suffix *1* and *2* stand for structure 1 and 2, respectively.

A. Open-Loop operation

When the *S* switch is turned on and off directly by the open loop control independently on the state variables and therefore the values τ_1 and $\tau_2=T_r-\tau_1$ are preset, the periodic state of the converter can be calculated as follows:

The value of the state vector at the end of structure 1 in the *k*th period from (5)

$$\underline{x}_{k1,e}=\underline{\underline{W}}_1(\tau_1)\underline{x}_{k1,s}+\underline{\underline{M}}_1(\tau_1)\underline{\underline{B}}_1\,\underline{g}(t)=\underline{x}_{k2,s} \tag{8}$$

The value of the state vector at the end of structure 2

$$\underline{x}_{k2,e}=\underline{\underline{W}}_2(\tau_2)\underline{x}_{k1,e}+\underline{\underline{M}}_1(\tau_1)\underline{\underline{B}}_1\,\underline{g}(t)=\underline{x}_{(k+1)1,s} \tag{9}$$

The $\underline{X}_s=\underline{x}_{k1,e}=\underline{x}_{(k+1)1,e}=\underline{X}_e$ is the steady state solution for known τ_1 and $\tau_2=T_r-\tau_1$

$$\underline{X}_s=\left[\underline{\underline{I}}-\underline{\underline{W}}_2(\tau_2)\underline{\underline{W}}_1(\tau_1)\right]^{-1}\left[\underline{\underline{W}}_2(\tau_2)\underline{\underline{M}}_1(\tau_1)\underline{\underline{B}}_1\,\underline{g}+\underline{\underline{M}}_2(\tau_2)\underline{\underline{B}}_2\,\underline{g}\right] \tag{10}$$

B. Closed-Loop operation

In closed-loop operation τ_1 is not known, however in steady-state both (3) and (10) hold true. Furthermore the start and the end value of the output of the PI controller must be the same $y_s=y_e$.

For determining τ_1, first $\underline{X}_s$ is calculated from (10) by an initially selected τ_1. Then from (1):

$$D(\tau_1)=y_e-y_s=-K_p\underline{k}_1^T(\underline{X}_e-\underline{X}_s)+\frac{K_p}{T_i}(\omega_{ref}T_r-$$

$$-\underline{k}_1^T\left(\int_0^{\tau_1}\underline{x}_1(\tau)d\tau+\int_0^{T_r-\tau_1}\underline{x}_2(\tau)d\tau\right) \qquad (11)$$

where $\underline{k}_1^T=[1\quad 0]$, $\underline{x}_j(\tau)=\underline{\underline{W}}_j(\tau)\underline{X}_j+\underline{\underline{M}}_j(\tau)\underline{\underline{B}}_j\underline{g}$, $\underline{X}_1=\underline{X}_s$ és $\underline{X}_2=\underline{X}(\tau_1)$. In steady-state $\underline{X}_e-\underline{X}_s$ is zero and it can be omitted. Likely $D(\tau_1)$ will not be zero at the first estimation of τ_1. The value of τ_1 can be determined by an iterative calculation using suitable mathematical software.

IV. Stability Analysis

The relation among the small deviations of the state vector around the fixed point $\underline{X}_s$ at the start of consecutive periods is

$$\Delta\underline{x}_{(k+1)1,s}=\underline{\underline{J}}_K\Delta\underline{x}_{k1,s}=\underline{\underline{J}}_K^k\Delta\underline{x}_{11,s} \qquad (12)$$

where $\Delta\underline{x}_{11,s}$ is the initial deviation of the perturbed state vector from $\underline{X}_s$ and $\underline{\underline{J}}_K$ is the Jacobian matrix. The stability criteria is that *the absolute value of the largest eigenvalues of* $\underline{\underline{J}}_K$ *has to be less than one.*

A. Extended System Matrixes

The integration property of the controller involves a new state variable. The output of the controller as a new state variable has to be included in the state vector $\underline{x}^{*T}=[\underline{x}^T\quad y]$. According to (1)

$$\dot{y}(t)=-K_p\dot{\Omega}+\frac{K_p}{T_i}(\Omega_{ref}-\Omega) \qquad (13)$$

The extended system matrix are

$$\underline{g}^{*T}=[\underline{g}^T\quad \Omega_{ref}],$$

$$\underline{\underline{A}}_j^*=\begin{bmatrix}\underline{\underline{A}}_j & & 0\\ & & 0\\ K_p(B/J-1/T_i) & -K_pK_T/J & 0\end{bmatrix}$$

$$\underline{\underline{B}}_j^*=\begin{bmatrix}\underline{\underline{B}}_j & 0\\ & 0\\ K_p/J & 0 \quad K_p/T_i\end{bmatrix}$$

Later on the marking * denotes vectors and matrices in the extended space.

B. Auxiliarly State Vector

The calculation of the Jacobian matrix is carried out by following the effects of a small initial perturbation. The deviation from the periodic trajectory during a T_r period is calculated by taking into consideration the change of the switching instance and its effect as well. As a result of an initial perturbation the state vector deviates from the steady-state space vector with $\Delta\underline{x}^*_{k1,e}(\tau_1)$ at the end of the structure 1 in period k (Fig.3). Simultaneously the switching instant τ_1 will change by $\Delta\tau_k$ as well. The actual state vector at the switching instant is $\underline{x}^*_{k1,e}(\tau_1+\Delta\tau_k)$. $\Delta\tau_k$ is changing from period to period.

The calculation of the Jacobian matrix is greatly facilitated by the introduction of an auxiliary state vector $\underline{x}^*_{k2,s}(\tau_1)$ and its change $\Delta\underline{x}^*_{k2,s}(\tau_1)$ instead of using $\underline{x}^*_{k1,e}(\tau_1+\Delta\tau_k)$ and $\Delta\underline{x}^*_{k1,e}(\tau_1+\Delta\tau_k)$ (see Fig.3) [3]. The auxiliary state vector points to a virtual initial state $D_3(\tau_1)$ where starting the system at τ_1 from, the dynamics of the structure 2 would drive the trajectory along the same orbit as the perturbed one after $\tau_1+\Delta\tau_k$.

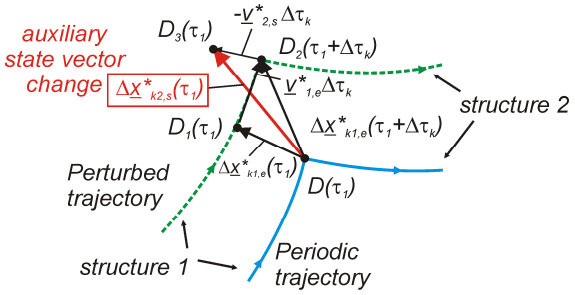

Figure 3. Auxiliary state vector change

The state vector change at τ_1 (between point D_1 and D)

$$\Delta\underline{x}^*_{k1,e}(\tau_1)=\underline{\underline{W}}^*_1(\tau_1)\Delta\underline{x}^*_{k1,s} \qquad (14)$$

The commutation between the two structures takes place at $\tau_1+\Delta\tau_k$ at the point D_2. The distance between D_1 and D_2 is $\underline{v}^*_{1,e}\Delta\tau_k$, where $\underline{v}^*_{1,e}$ is the velocity of the state vector at τ_1 in the structure *1*. After the switching the velocity at the start of the structure *2* is $\underline{v}^*_{2,s}$. Due to the linearity of the structures the new trajectory can be projected backward in time from time $\tau_1+\Delta\tau_k$ to τ_1. In other words the trajectory will start from the point D_3 rather than the point D_2 by extending the new trajectory at the start of the structure 2 toward the negative time in the direction of the velocity vector $-\underline{v}^*_{2,s}$. The point D_3 is reached this way at the distance $-\underline{v}^*_{2,s}\Delta\tau_k$ from D_2. The auxiliary state vector change is obtained between D_3 and D. Now the applying $\Delta\underline{x}^*_{k2,s}(\tau_1)$ instead of $\Delta\underline{x}^*_{k1,e}(\tau_1+\Delta\tau_k)$ the trajectory will start in the structure *2* at the same τ_1 instant as in the case of the periodic trajectory prior perturbation.

From Fig.3 the auxiliary state vector change:

$$\Delta\underline{x}^*_{k2,s}(\tau_1)=\Delta\underline{x}^*_{k1,e}(\tau_1)+(\underline{v}^*_{1,e}-\underline{v}^*_{2,s})\Delta\tau_k \qquad (15)$$

where the velocities of the state vectors can be calculated from (4). By using the auxiliary state vector, $\Delta\tau_k$ are taken

into consideration and we are permitted to use τ_1 and $\tau_2=T_r-\tau_1$ as well as $\underline{\underline{W}}_1^*(\tau_1)$ and $\underline{\underline{W}}_2^*(\tau_2)$.

C. Calculation of $\Delta\tau_k$

According to (3) the switching condition for periodic trajectory is

$$\underline{k}_3^{*T}\,\underline{x}^*(\tau_1)-A_i\,\underline{k}_2^{*T}\,\underline{x}^*(\tau_1)=0 \tag{16}$$

and for perturbed trajectory

$$\underline{k}_3^{*T}(\underline{x}^*(\tau_1)+\Delta\underline{x}_{k1,e}^*(\tau_1+\Delta\tau_k))- \\ -A_i\,\underline{k}_2^{*T}(\underline{x}^*(\tau_1)+\Delta\underline{x}_{k1,e}^*(\tau_1+\Delta\tau_k))=0 \tag{17}$$

where $k_2^{*T}=[0\quad 1\quad 0]$ and $k_3^{*T}=[0\quad 0\quad 1]$. From triangle DD_1D_2 (Fig. 3) follows

$$\Delta\underline{x}_{k1,e}^*(\tau_1+\Delta\tau_k)=\Delta\underline{x}_{k1,e}^*(\tau_1)+\underline{v}_{1,e}^*\Delta\tau_k \tag{18}$$

Subtracting (16) from (17) and substituting $\Delta\underline{x}_{k1,e}^*(\tau_1+\Delta\tau_k)$ into the result, $\Delta\tau_k$ can be expressed

$$\Delta\tau_k=\frac{(\underline{k}_3^{*T}-A_i\,\underline{k}_2^{*T})}{(A_i\,\underline{k}_2^{*T}-\underline{k}_3^{*T})\underline{v}_{1,e}^*}\Delta\underline{x}_{k1,e}^*(\tau_1) \tag{19}$$

Substituting $\Delta\tau_k$ from here into (15)

$$\Delta\underline{x}_{k2,s}^*(\tau_1)=(\underline{\underline{I}}+\frac{(\underline{v}_{1,e}^*-\underline{v}_{2,s}^*)(\underline{k}_3^{*T}-A_i\,\underline{k}_2^{*T})}{A_i\,\underline{k}_2^{*T}\,\underline{v}_{1,e}^*-\underline{k}_3^{*T}\,\underline{v}_{1,e}^*})\Delta\underline{x}_{k1,e}^*(\tau_1)= \\ =\underline{\underline{M}}\Delta\underline{x}_{k1,e}^*(\tau_1) \tag{20}$$

D. Jacobian matrix

Applying the previous equations

$$\Delta\underline{x}_{(k+1)1,s}^*=\Delta\underline{x}_{k2,e}^*=\underline{\underline{W}}_2^*(\tau_2)\Delta\underline{x}_{k2,s}^*=\underline{\underline{W}}_2^*(\tau_2)\underline{\underline{M}}\Delta\underline{x}_{k1,e}^*(\tau_1)= \\ =\underline{\underline{W}}_2^*(\tau_2)\underline{\underline{M}}\underline{\underline{W}}_1^*(\tau_1)\Delta\underline{x}_{k1,s}^*=\underline{\underline{J}}_K\Delta\underline{x}_{k1,s} \tag{21}$$

For a given τ_1 and $\tau_2=T_r-\tau_1$ value the Jacobian matrix can be calculated from

$$\underline{\underline{J}}_K=\underline{\underline{W}}_2^*(\tau_2)\underline{\underline{M}}\underline{\underline{W}}_1^*(\tau_1) \tag{22}$$

V. Control of Chaos

The DC drive has a very colorful response depending on its parameters (see next section). Its behavior can be chaotic from the stable period-1 operation through bifurcation cascade. By using the stability analysis method derived in previous section the controller parameters (K_p, T_i, A_i) can be calculated to maintain a stable operation at the rated parameters. However, sudden changes in the input signals (like loading torque, reference signal and input voltage) can result that the largest eigenvalue of $\underline{\underline{J}}_K$ leaves the unit circle resulting an unstable operation.

To widen the stable domain a periodic ramp signal with period T_r synchronized to clock pulse is added to the current loop (see Fig.1 dotted line). By properly selected slope of the signal the DC drive can be stable in the whole operating range.

The equation of the current loop during one T_r period is changed to

$$u(\tau)=A_i i(\tau)+m_c\frac{\tau}{T_r} \tag{23}$$

This change has to be taken into consideration in (16) and (17) to calculate $\Delta\tau_k$, which results that $\underline{\underline{M}}$ will be

$$\underline{\underline{M}}'=(\underline{\underline{I}}+\frac{(\underline{v}_{1,e}^*-\underline{v}_{2,s}^*)(\underline{k}_3^{*T}-A_i\,\underline{k}_2^{*T})}{A_i\,\underline{k}_2^{*T}\,\underline{v}_{1,e}^*-\underline{k}_3^{*T}\,\underline{v}_{1,e}^*+\frac{m_c}{T_r}}) \tag{24}$$

It is obvious that by increasing m_c the eigenvalues of the Jacobian matrix decrease provided that $\underline{\underline{W}}_1^*(\tau_1)$ and $\underline{\underline{W}}_2^*(\tau_2)$ are the same matrices (see (22)). For a given operation range of the DC drive the required value of m_c to keep the largest eigenvalue of the Jacobian matrix in the unit circle can be calculated.

VI. Simulation Results

To illustrate the stability calculation and the method of control of chaos computer simulation were carried out in MATLAB/Simulink environment. The rated simulation parameters were $B = 0.000275$ Nm/rad/s, $J = 0.000557$ Nms^2, $K_E = 0.1324$ V/rad/s, $K_T = 0.1324$ Nm/A, $R_a = 2.9\Omega$, $L_a = 0.0537$ H, $V_{in} = 60$ V, $T_{load} = 0.39$ Nm, $A_i = 1$, $K_p = 2$, $T_i = 0.1$ s, $\Omega_{ref} = 105$ rad/s and the period of clock signal is $T_r = 0.002$ s.

The selected switching frequency is quite low compare to the values applied in practical dc drives. The reason of the selected switching frequency is to emphasize the nonlinear behavior of the speed control loop.

Figure 4 shows the response of the drive system near different K_p value. Figure 4a shows the stable period-1 orbit. The absolute value of the largest eigenvalues of the Jacobian matrix now is $\lambda=0.98$. By increasing the proportional gain the largest eigenvalue of the Jacobian

matrix leaves the unit circle. Figure 4b and c show an unstable period-2 and period-4 orbit, when $\lambda=1.23$ and 1.56, respectively. For $K_p=5.2$ the system is in chaos (Fig.4d., $\lambda=1.78$) and the speed time function never repeats itself.

An overall picture of the behavior of a nonlinear system is offered by the bifurcation diagram showing the various states and the sudden changes or bifurcations of the system due to the variation of thebifurcation parameter. For this case the bifurcation diagram is obtained by sampling the speed $\Omega\ (t)$ and the current $i(t)$ signal at the start of every switching period in "steady state" and plotting these sampled values $\Omega_k=\Omega\ (kT_r)$ or $i_k=i(kT_r)$ as a function of the bifurcation parameter. Figure 5a and b shows the bifurcation diagram of the drive when the bifurcation parameter is K_p and V_{in}, respectively. The sampled Ω_k of the time functions shown in Fig.4 are denoted by a circle in Fig.5a.

As it can be seen on the simulation results - unlike linear systems - changes in the variables can result different responses. To maintain stable period-1 state in the whole operation range a ramp signal is added to the current control loop as it was mentioned in the previous

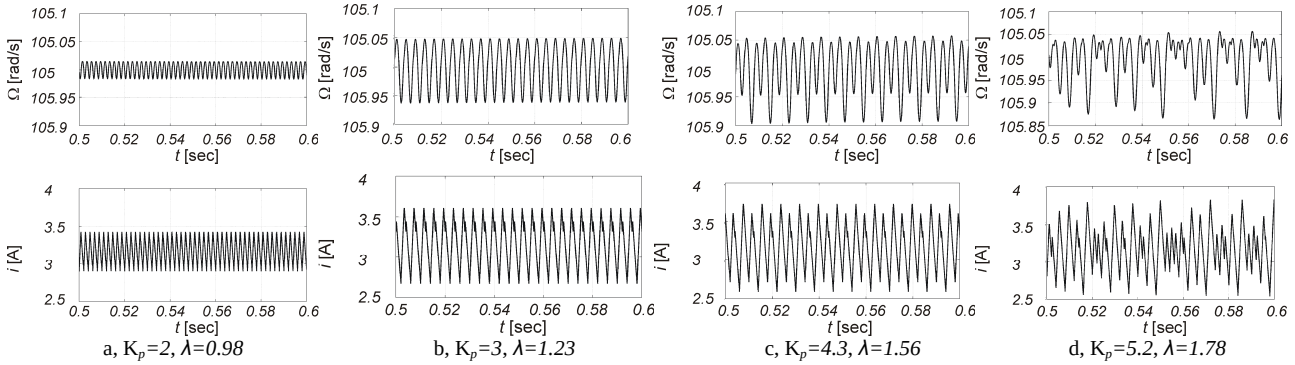

a, $K_p=2$, $\lambda=0.98$ b, $K_p=3$, $\lambda=1.23$ c, $K_p=4.3$, $\lambda=1.56$ d, $K_p=5.2$, $\lambda=1.78$

Figure 4. $\omega(t)$ and $i(t)$ near different load

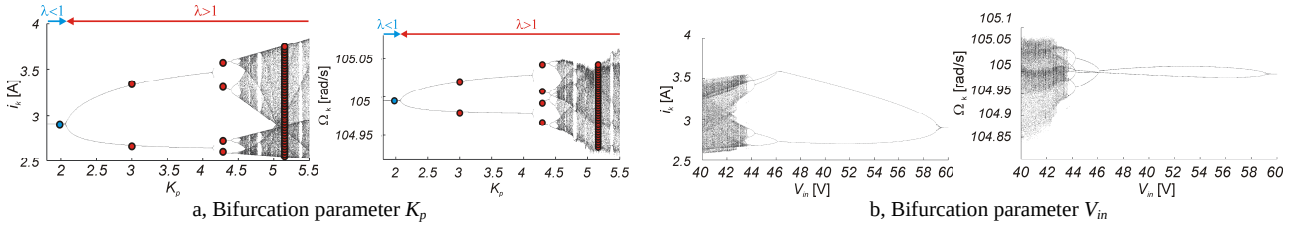

a, Bifurcation parameter K_p b, Bifurcation parameter V_{in}

Figure 5. Bifurcation diagram for T_{load} (a) and K_p (b)

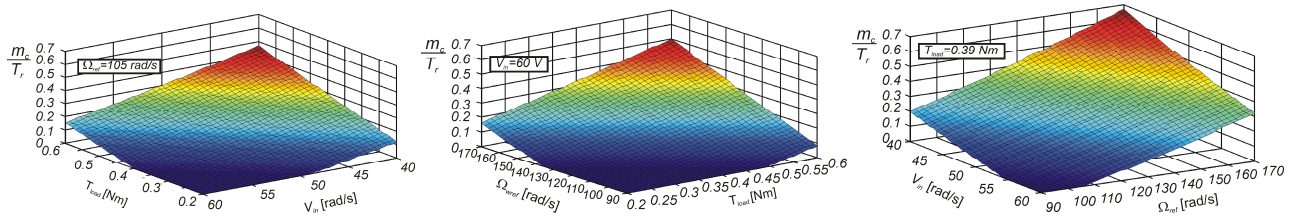

a, m_c as a function of V_{in} and T_{load} b, m_c as a function of ω_{ref} and T_{load} c, m_c as a function of V_{in} and ω_{ref}

Figure 6. Required slope value of the ramp signal

section. The operating range of the drive system is selected as T_{load} = *0.2-6* Nm, V_{in} = *40-60* V, Ω_{ref} = *90-170* rad/s. The other parameters of the drive assumed being constant during the operation.

Based on the section V the required m_c slope of the ramp signal was determined in the whole operation range of the drive (Fig. 6). From the figures it can be concluded by selecting m_c/T_r=0.7, the drive system is stable for changes in the whole operation range.

To illustrate the effect of the ramp compensation (RC) Fig.7 shows the time functions of the speed and the current of the drive, when Ω_{ref} =*120 rad/s*, T_{load} = *0.54* Nm and V_{in} = *50* V. The motor without RC (light grey line) has a chaotic response with large ripples. The value of the largest eigenvalues of the Jacobian matrix is $\lambda=1.89$. By increasing the switching frequency to f_c = *1* kHz, the ripple both in the speed and the current is reduced, however the response is still chaotic (dark grey line, $\lambda=1.6$). By applying RC with slope m_c/T_r=0.7 to keep λ in the unit circle (black line) near the lower nominal switching frequency a stable response can be obtained with the same ripple in the speed and currents as at higher switching frequency.

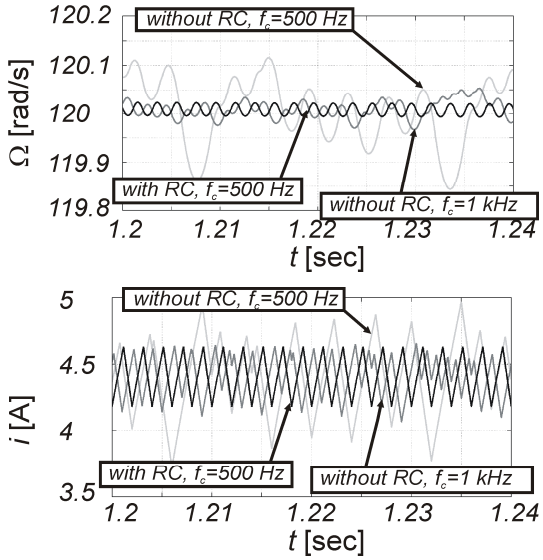

Figure 7. *Effect of chaos control loop*

VII. CONCLUSIONS

The paper presents the utilization of the auxiliary state vector to determine the stability border of a DC drive system. The derivation of the Jacobian matrix without the Poincaré Map Function is explained.

The unstable and chaotic response of the drive can be avoided by a ramp signal applied in the current loop. The required slope of the ramp signal was determined also with the auxiliary state vector.

The numerical results of the calculations were verified by computer simulations.

ACKNOWLEDGMENT

This paper was supported by the Hungarian Research Fund (OTKA K72338) and the Control Research Group of the Hungarian Academy of Sciences (HAS) furthermore the Hungarian Science and Technology Foundation in framework of IT-20/2007 project. This work is connected to the scientific program of the "Development of quality-oriented and cooperative R+D+I strategy and functional model at BME" project.

REFERENCES

[1] K. T. Chau, Z. Wang, "Chaos in Electric Drive Systems, Analysis, Control and Applications", 2011, John Wiley & Sons (Asia), ISBN: 978-0-470-82633-1

[2] Banerjee S. and Verghese G., Nonlinear Phenomena in Power Electronics: Attractors, Bifurcations, Chaos, and Nonlinear Control. New York.: IEEE Press, 2001.

[3] Octavian Dranga, Balázs Buti, István Nagy, Hirohito Funato: "Stability Analysis of Nonlinear Power Electronic Systems Utilizing Periodicity and Introducing Auxiliarly State Vector", IEEE Transactions on Circuit and Systems-I, Regular Papers, Vol.52, No.1, 2005 January, pp168-178

[4] N. C. Okafor, D. Giaouris, B. Zahawi, S. Banerjee: „Analysis of fast-scale Instability in DC Drives with Full-Bridge Converter using Filippov's method", Power Electronics, Machines and Drives, PEMD, 19-21 April 2010, pp1-5

[5] D. Dai, X. Ma, B. Zhang, CK. Tse, "Hopf Bifurcation and Chaos from Torus Breakdown in Voltage-Mode Controlled DC Drive Systems" Elsevier, Chaos, Solitons and Fractals, 2008

[6] S. Banerjee, "Is the Knowledge about Bifurcation and Chaos in Power Electronics Useful in Practice?" IEEE International Conference on Industrial Technology, ICIT, 15-17. Dec. 2006, pp. 943-1948

[7] H. H. C. Iu, B. Robert, "Control of chaos in a PWM current-mode H-brdige inverter using time-delayed feedback", IEEE Transactions on Circuits and Systems – I, Vol. 50, No. 8, August 2003, pp1125-1129

[8] A. E. Aroudi, M. Orabi, "Stabilizing Technique for AC-DC Boost PFC Converter Based on Time Delay Feedback, IEEE Transactions on Circuits and Systems – II, Vol.57, No.1, January 2010, pp56-60

[9] B. Bao, G. Zhou, J. Xu, Z. Liu, "Unified Classification of Operation State Regions for Switching Converters with Ramp Compensation", IEEE Transactions on Power Electronics, Vol.26, No. 7., July 2011, pp1968-1975

[10] El Aroudi A, Angulo F, Olivar G, Robert BGM, Feki M, "Stabilizing a two-cell DC-DC Buck Converter by Fixed Point Induced Control" International Journal of Bifurcation and Chaos, Vol. 19, Issue 6, 2009, pp. 2043-2057

[11] D. Giaouris, S. Banerjee, B. Zahawi, V. Pickert "Control of Fast Scale Bifurcation in Power-Factor Correction Converters" IEEE Transactions on Circuits and Systems–II: Express Briefs, Vol.54, No.9, September, 2007, pp. 805-809

[12] Sergey Ryvkin, "Cutting out the Voltage Oscillation Influence on the Control Quality of a Three-Level Inverter Drive by Using Sliding Mode" EPE-PEMC 2010, 6-8 September, 2010, Ohrid, Republic of Macedonia, pp. T3-6-T3-12, CD Rom ISBN: 978-1-4244-7854-5

[13] J. Leuchter, P. Bauer, V. Rerucha, V. Hajek, "Dynamic Behavior Modeling and Verification of Advanced Electrical-Generator Set Concept" IEEE Transactions on Industrial Electronics, January, 2009, vol. 56, nr:1, pp. 266-279

[14] V. Moreno-Font, A. El Aroudi, J. Calvente, R. Giral, L. Benadero, "Dynamics and Stability Issues of a Single-Inductor Dual-Switching DC-DC Converter" IEEE Transactions on Circuits and Systems-I: Regular Papers, Vol 57, No. 2, February 2010, pp.415-426

[15] Kolokolov Y, Ustinov P, Essounbouli N, Hamaoui A, "Bifurcation-free design method of pulse energy converter controllers", Chaos Solitons and Fractals, Vol.42, No.5, 2009, pp. 2635-2644

[16] V. Ruscin, M. Lacko, M. Olejar, J.Dudrik, "Soft Switching PS-PWM DC-DC Converter Controlled by Microprocessors", EDPE'07, High Tatras, Slovakia, 24 -26 Sept, 2007, CD rom ISBN: 978-80-8073-868-6

[17] Aroudi, B. Robert, L. Martinez-Salamero, "Bifurcation Behavior of a Three Cell DC-DC Buck Converter", EPE-PEMC'06, Portoroz, Slovenia, August 30- September 01, 2006, pp. 1994-2001, CD Rom ISBN: 1-4244-0121-6

[18] Z. Ye, P. K. Jain, P. Sen, "Phasor-Domain Modeling of Resonant Inverters for High-Frekvency AC Power Distribution Systems ", IEEE Trans. on Power Electronics. Vol 24, No. 4, April 2009, pp. 911-923

[19] J.F. Baalbergen, P. Bauer, JA Ferreira, "Energy Storage and Power Management for Typical 4Q-load", IEEE Transactions on Industrial Electronics, Vol.56, No.5, 2009, pp.1485-1498

[20] P.M. Lacko M. Olejar, J. Dudrik, "DC-DC Push – Pull Converter with Turn-Off Snubber for Renewable Energy Sources", EDPE 2009, Dubrovnik, Croatia, 12-14 Oct, 2009, CD Rom ISBN: 953-6037-56-8

[21] V. Oleschuk, F. Profumo, A. Tenconi. „Simplifying Approach for Analysis of Space-Vector PWM for Three-Phase and Multiphase Converters" EPE'07, Aalborg, Denmark, 2-5 szept, 2007, CD Rom ISBN: 9789075815108

[22] J. Dudrik, J. Oetter, "High-Frequency Soft-Switching DC-DC Converters for Voltage and Current DC Power Sources", Acta Polytecnica Hungerica, Vol. 4, Issue 2, ISSN 1785-8860 2007, pp. 29-46

[23] C. Sreecumar, V. Agarwal, "Hybrid Control Approach for the Output Voltage Regulation in Buck Type DC-DC Converter", IET Electric Power Applications, 2007, Vol. 1, Issue 6, pp. 897- 906

[24] L. Benadero, V. Moreno, " A Qualitative Analysis of Non-Smooth Bifurcations of Low-Frequency Oscillations in a PWM Boost Converter Using Averaging Approaches ",EPE-PEMC 2004 Riga, Latvia, 2-4 September, 2004, CD Rom ISBN: 9984-32-034-0,

THE AUTHORS

Peter Stumpf received the M.Sc. degree from the Budapest University of Technology and Economics (BUTE), Budapest, Hungary, in 2009, where he is currently working toward the Ph.D. degree. His research interests focus on power electronics, nonlinear dynamics and modulation strategies. He is co-author of 12 technical papers.

István Nagy received the M.Sc and PhD degrees from BUTE. He was employed in the Ganz Electric Factory, later as Department Head in a Research Institute of the Hungarian Academy of Sciences (HAS). He became full professor at BUTE in 1975. He was visiting professor at universities in Germany, India, New Zealand, Italy, Canada, USA and Japan. His current research interests are power electronics, automatic electric drives, variable structure nonlinear systems, nonlinear dynamics. He is author or co-author of 8 textbooks, 5 handbooks, around 300 technical papers and 13 patents. He was leader or participant in R&D work of considerable number of industrial products. He is member of the HAS, IEEE Fellow, chairman of EPE-PEMC Council, President of the Hungarian CIGR Committee, member of the Hungarian IEE, EPE. He served in various Committees in IEEE.